Available online at www.sciencedirect.com
SCIENCE DIRECT®
Biochemical Pharmacology 65 (2003) 1227–1241
Biochemical Pharmacology
www.elsevier.com/locate/biochempharm

Comparison of the pharmacological antagonism of M_2 and M_3 muscarinic receptors expressed in isolation and in combination

Michael T. Griffin[a], Jake Ching-Hsuan Hsu[b], Darakhshanda Shehnaz[b], Frederick J. Ehlert[b,*]

[a]*Department of Environmental and Chemical Sciences, Chapman University, Orange, CA 92866, USA*
[b]*Department of Pharmacology, College of Medicine, University of California, Irvine, CA 92697-4625, USA*

Received 23 May 2002; accepted 9 September 2002

Abstract

We compared the binding properties of selective muscarinic antagonists with their potencies for antagonizing muscarinic responses in Chinese hamster ovary (CHO) cells expressing M_2 and M_3 muscarinic receptors in combination and in isolation. When measured by the competitive displacement of [^{3}H]*N*-methylscopolamine binding to CHO cells expressing both M_2 and M_3 muscarinic receptors (CHO $M_2 + M_3$ cells), the competition curves of the subtype-selective muscarinic antagonists were consistent with a two-site model. One site exhibited binding properties identical to those of CHO M_2 cells, whereas the other site exhibited properties like those of CHO M_3 cells. Oxotremorine-M, a muscarinic agonist, elicited a robust, pertussis toxin-insensitive stimulation of phosphoinositide hydrolysis in both CHO M_3 and CHO $M_2 + M_3$ cells, but not in CHO M_2 cells. The pharmacological antagonism of the phosphoinositide response exhibited similar properties in both CHO M_3 and CHO $M_2 + M_3$ cells. Oxotremorine-M elicited a pertussis toxin-sensitive, robust inhibition of forskolin-stimulated cyclic AMP (cAMP) accumulation in both CHO M_2 and CHO $M_2 + M_3$ cells and a less robust inhibition in CHO M_3 cells. At higher concentrations, oxotremorine-M elicited an increase in cAMP accumulation over the maximal inhibition noted at lower concentrations in both CHO M_3 and CHO $M_2 + M_3$ cells. Following pertussis toxin treatment, only the stimulatory phase of the cAMP response to oxotremorine-M was observed in CHO M_2, CHO M_3, and CHO $M_2 + M_3$ cells. The pharmacological antagonism of the cAMP response in CHO $M_2 + M_3$ cells resembled that expected for a response mediated independently by both M_2 and M_3 receptors.

Keywords: Muscarinic receptors; Coexpression; Cyclic AMP; Adenylyl cyclase; Phosphoinositide hydrolysis; Pertussis toxin

1. Introduction

Selective competitive antagonists can be useful probes for exploring the functional role of receptor subtypes in various physiological responses. Because many such agents exhibit limited selectivity, it is often impossible to identify a single blocking concentration of an antagonist that would greatly inhibit responses elicited by one receptor subtype, without also inhibiting to a certain extent responses elicited by other subtypes. Moreover, the degree of inhibition would change depending upon the concentration of agonist or the amount of endogenous neurotransmitter released. If a response to an exogenously applied agonist is being measured *in vitro*, a more powerful approach is to measure the shift in the agonist concentration–response curve caused by the competitive antagonist [1]. With this strategy, the dissociation constant of the antagonist (K_b value) for the receptor that mediates the response can be estimated using standard competitive inhibition relationships. This K_b value should agree with the K_d value of the antagonist measured in a binding assay on a cell line expressing the same recombinant receptor. By repeating this measurement with a handful of antagonists, it should be possible to identify the receptor mediating the response with certainty.

A potential complication with this approach is that the agonist may elicit the response in question by interacting with more than one receptor subtype. Under this circumstance, it is still possible to glean information about the receptors contributing to the response provided that an appropriate model for the interaction is considered. It is also possible that the receptors themselves may interact with one another to form a heteromeric receptor complex

* Corresponding author. Tel.: +1-949-824-6208; fax: +1-949-824-4855.
E-mail address: fjehlert@uci.edu (F.J. Ehlert).

Abbreviations: cAMP, cyclic AMP; CHO, Chinese hamster ovary; 4-DAMP mustard, *N*-2-chloroethyl-4-piperidinyl diphenylacetate; KRB, Krebs–Ringer bicarbonate; NMS, *N*-methylscopolamine.

0006-2952/03/$ – see front matter
doi:10.1016/S0006-2952(03)00068-6

exhibiting a unique pharmacology. This situation has been shown to occur with δ- and γ-opioid receptors [2].

To examine the feasibility of comparing antagonist binding affinity with functional antagonism, we investigated the pharmacological antagonism of muscarinic responses in CHO cells transfected with muscarinic M_2 and M_3 receptors in isolation, as well as in combination. These two receptor subtypes are expressed abundantly in smooth muscle where they signal through G_i and G_q, respectively [3,4]. Our results show (a) good agreement between the binding affinity of muscarinic antagonists and their antagonism of muscarinic responses, and (b) that the pattern of coupling of M_2 and M_3 receptors to adenylyl cyclase and phospholipase-Cβ is similar when these receptors are expressed in isolation or in combination.

2. Materials and methods

2.1. Cell culture

Clonally selected CHO cells expressing either the human M_2 muscarinic receptor (CHO M_2 cells) or the human M_3 receptor (CHO M_3 cells) were cultured as previously described [5] in growth medium (DMEM, high glucose plus L-glutamine, 7% fetal bovine serum, and 100 units/mL of penicillin and streptomycin) supplemented with 225 μg/mL of neomycin (G 418 sulfate). CHO cells expressing both human M_2 and M_3 muscarinic receptors (CHO $M_2 + M_3$ cells) were cultured in the same growth medium described above but supplemented with 400 μg/mL of hygromycin-B.

2.2. Transfection of CHO M_3 cells with M_2 muscarinic receptors

An Okayama-Berg expression vector pCD1 containing the human M_2 sequence (M_2 pCD clone) and CHO cells stably transfected with either the M_2 or the M_3 muscarinic receptor subtypes were provided by Tom Bonner (NIH) and Mark Brann (Acadia Pharmaceuticals), respectively. Since the M_2 pCD expression vector contained the same selection marker (neomycin) as the CHO M_3 cell line, the coding portion of the M_2 gene was excised and inserted into a hygro(–)pcDNA3.1 expression vector (Invitrogen) and then transfected into the CHO M_3 cell line. The portion of the M_2 pCD vector spanning between the *Xho*I (nucleotide 5738) and the *Kpn*I (nucleotide 1737) restriction sites, which contains the coding sequence of the M_2 receptor, was inserted between the corresponding sites of the multiple cloning site of the hygro(–)pcDNA3.1 vector using T4 ligase. Digestion with *Apa*I confirmed that the M_2 sequence was inserted with proper orientation. CHO M_3 cells were transfected with the M_2 pcDNA3.1/hygro(−) vector using Lipofectamine. Hygromycin-resistant colonies were submitted to three rounds of clonal selection and screened for M_2 receptor expression using a whole cell-binding assay with the muscarinic antagonist [^{3}H]NMS, which binds to both M_2 and M_3 muscarinic receptors. The selection procedure is based upon the sensitivity of cellular [^{3}H]NMS binding to prior treatment with 4-DAMP mustard. 4-DAMP mustard is an irreversible alkylating agent that selectively inactivates M_3 receptors over M_2, particularly when the alkylation procedure is carried out in the presence of a competitive M_2 selective antagonist, like [[2-[(diethylamino)methyl]-1-piperidinyl]acetyl]-5,11-dihydro-6*H*-pyrido-[2,3-b][1,4]-benzodiazepine-6-one (AF-DX 116) [6]. CHO cells expressing a substantial population of 4-DAMP mustard-insensitive [^{3}H]NMS binding sites were selected as M_2 receptor expressing cells.

2.3. [^{3}H]NMS binding to intact cells

CHO cells expressing muscarinic receptors were cultured to confluence in 24-well plates (Costar). Cells were washed with an aliquot (0.5 mL) of KRB buffer (124 mM NaCl, 5 mM KCl, 1.3 mM $MgCl_2$, 1.2 mM KH_2PO_4, 26 mM $NaHCO_3$, 1.8 mM $CaCl_2$, and 10 mM glucose) and then preincubated with 4 μM AF-DX 116 for 10 min at 37° and 5% CO_2/95% air. The medium was aspirated and cells were incubated with either 4 μM AF-DX 116 or 4 μM AF-DX 116 plus 40 nM 4-DAMP mustard for 1 hr at 37° in an atmosphere of 5% CO_2/95% air. Prior to use, 4-DAMP mustard was cyclized to its aziridinium ion by incubating a 0.4 mM solution of the parent mustard for 30 min at 37° in 10 mM $NaKPO_4$, pH 7.4, as described previously [6]. The solution was placed on ice and used as soon as possible. Cells were washed twice with 0.5 mL of KRB buffer and then incubated in a final volume of 1 mL of KRB buffer containing [^{3}H]NMS (0.5 nM) for 1 hr at 37° and 5% CO_2. Non-specific binding was defined as that measured in the presence of 10 μM atropine. Following two washes with ice-cold KRB buffer, 0.5 mL of 0.25 N NaOH was added to each well. After 30 min, the cell digest was neutralized with 2.5 N HCl and transferred to scintillation vials for estimation of radioactivity.

2.4. [^{3}H]NMS binding to cellular homogenates

Confluent CHO cells were detached from 150-mm dishes by incubation at 37° for 5 min in 2.5 mL of a normal saline solution containing trypsin (500 μg/mL) and EDTA (200 μg/mL). The harvested cells were washed once in saline solution, centrifuged at 2000 *g* for 5 min at 4°, and the pellets frozen at −20°. Frozen cells were resuspended in modified KRB buffer (124 mM NaCl, 5 mM KCl, 3 mM $MgSO_4$, 26 mM $NaHCO_3$, 10 mM Na/Hepes, pH 7.4) and then homogenized with a Potter–Elvehjem glass homogenizer with a Teflon pestle. Cellular homogenates were incubated for 1 hr at 30° in a final volume of 1 mL of modified KRB buffer containing [^{3}H]NMS and, when present, various concentrations of muscarinic antagonists. All assays were run in triplicate, and non-specific binding

was defined as the residual binding in the presence of 10 μM atropine.

In some experiments, binding assays were run on cellular homogenates that had been incubated with 4-DAMP mustard and then washed extensively. For these experiments, frozen cells were resuspended in modified KRB buffer and homogenized with a Polytron homogenizer (Brinkmann Instruments) at setting #5 for 10 s. The homogenate was divided into two equal volumes and incubated for 5 min at 37° in the presence of AF-DX 116 (4 μM). An aliquot of cyclized 4-DAMP mustard (final concentration of 40 nM) was added to one of the homogenates, whereas the other served as the control. Both homogenates were incubated for 1 hr at 37°. The reaction with 4-DAMP mustard was stopped by the addition of $Na_2S_2O_4$ at a final concentration of 1 mM followed by an additional 10-min incubation at 37°. Homogenates were centrifuged at 30,000 *g* for 10 min at 4°, resuspended in fresh modified KRB buffer, and then centrifuged once more as just described. Pellets were resuspended in modified KRB buffer and incubated in a final volume of 1 mL containing various concentrations of [^{3}H]NMS for 1 hr at 25°.

The binding of [^{3}H]NMS to cellular homogenates was measured by the filtration method [7] using a cell harvester, which trapped membrane-bound [^{3}H]NMS on Whatman GF/B glass fiber filters (Brandel). Before use, the filters were soaked on 0.1% polyethyleneamine–HCl, pH 7.4. After filtration of the assay tubes, the filters were rinsed with three aliquots (4 mL each) of ice-cold saline, and the trapped radioactivity was measured by liquid scintillation counting. Non-specific binding was defined as that measured in the presence of atropine (10 μM).

2.5. Phosphoinositide hydrolysis

Oxotremorine-M-stimulated phosphoinositide hydrolysis was measured in CHO cells transfected with muscarinic receptor subtypes using a modification of the [^{3}H]inositol-prelabeling method of Berridge *et al.* [8]. Our method employed the perchloric acid extraction procedure of Kendall and Hill [9]. Confluent monolayers grown in 24-well plates were washed with 0.5 mL of Minimal Essential Medium (MEM) with Earle's salts, L-glutamine, and bicarbonate buffer and then incubated overnight at 37° in 0.5 mL MEM containing 2.3 μCi [^{3}H]inositol in an atmosphere of 5% CO_2/95% air (16–18 hr). For antagonist competition studies, [^{3}H]inositol-treated cells were washed twice with 0.5 mL MEM and then preincubated with 10 mM LiCl and the antagonist for 20 min at 37° (5% CO_2/95% air). Medium was aspirated, and the assay was initiated by the addition of 0.5 mL MEM containing 10 mM LiCl, the antagonist, and various concentrations of oxotremorine-M. Following a 20-min incubation at 37° (5% CO_2/95% air), the reaction was stopped by removal of the medium and addition of 0.4 mL of ice-cold 2.5% (w/v) $HClO_4$. After at least 20 min on ice, an aliquot (0.9 mL) of 0.11 M KOH plus 0.01 M Tris base was added to each well, and the samples were incubated on ice for 15 min, but no longer. An aliquot (0.15 mL) of 0.5 M Tris–HCl, pH 7.4, was added, and the contents of each well were transferred to plastic tubes with an additional 0.5 mL wash volume. Cell extracts were centrifuged at 3000 *g* for 10 min at room temperature, and the supernatant was applied to a column of 1 mL of Dowex (AG1-X8, formate form, 100–200 mesh) at room temperature. After four washes, each with 5 mL of water, total [^{3}H]inositolphosphates were eluted into scintillation vials by the addition of 2.5 mL of 1 M ammonium formate and 0.1 M formic acid. Scintillation fluid (12 mL) was added to the vials, and radioactivity was measured for determination of [^{3}H]inositolphosphates. In experiments with pertussis toxin, the toxin (0.1 μg/mL; final concentration) was added to cell monolayers at the beginning of the overnight incubation with [^{3}H]inositol. In experiments with 4-DAMP mustard, cells were washed twice with 0.5 mL MEM (37°) following the overnight incubation in [^{3}H]inositol and then preincubated with MEM plus 4 μM AF-DX 116 for 15 min at 37° (5% CO_2/95% air). Medium was aspirated and replaced with 0.5 mL MEM plus 4 μM AF-DX 116 containing either 40 nM activated 4-DAMP mustard (cyclized to the aziridinium ion by a 30-min incubation at 37° in 10 mM $NaKPO_4$, pH 7.4) or vehicle. Following a 1-hr incubation at 37° in 5% CO_2/95% air, the cells were washed with MEM (0.5 mL) and used as described above.

In some experiments, phosphoinositide hydrolysis was measured using a continuous labeling paradigm. Cell monolayers were washed with 0.5 mL MEM and then incubated at 37° in 5% CO_2/95% air with 0.5 mL MEM containing various concentrations of oxotremorine-M and muscarinic antagonist. After 30 min, an aliquot (50 μL) containing [^{3}H]inositol (2 μCi) and LiCl (10 mM, final concentration) was added to each well. At the end of a 45-min incubation, the cells were washed once with 0.5 mL MEM containing 10 mM LiCl and then digested in 0.4 mL of 2.5% (w/v) $HClO_4$. Total [^{3}H]inositolphosphates were measured as described above.

2.6. cAMP accumulation

Oxotremorine-M-mediated inhibition of forskolin-stimulated cAMP accumulation was measured in CHO cells using a modification of the [^{3}H]adenine-prelabeling method of Schultz *et al.* [10]. Confluent cell monolayers were washed with 0.5 mL MEM and then incubated in 0.3 mL MEM containing 2 μCi [^{3}H]adenine and 30 μM adenine for 1 hr at 37° in an atmosphere of 5% CO_2. After two washes with 0.5 mL MEM, cells were preincubated with 0.5 mL MEM plus 0.5 mM 1-methyl-3-isobutylxanthine (IBMX) for an additional 12 min (37°, 5% CO_2/95% air). The reaction was started by replacing the medium with an aliquot (0.5 mL) of MEM containing IBMX (0.5 mM), forskolin (10 μM), and various concentrations of oxotremorine-M. The plates were

incubated at 37° for 12 min in 5% CO_2/95% air. In antagonist competition studies, the antagonist was included in both the preincubation and the incubation with oxotremorine-M. The reaction was stopped by aspiration of the reaction mixture followed by the addition of 0.5 mL of ice-cold 9% (w/v) trichloroacetic acid (TCA). After at least 30 min on ice, the contents of each well were transferred to plastic tubes together with an additional 0.5 mL wash of 9% TCA. The pooled TCA extracts were applied to a column of 1.5 mL Dowex (AG-50W-X4, 200-400 mesh) and washed with two aliquots of water (1.5 mL each) to remove [^{3}H]ATP. [^{3}H]cAMP was eluted onto a column of neutral alumina (0.6 g) with 5 mL of water and then eluted into scintillation vials with 4 mL of 0.1 M imidazole HCl (pH 7.5), and radioactivity was measured. In experiments with pertussis toxin, the toxin (0.1 μg/mL; final concentration) was added to cell monolayers 16–18 hr before [^{3}H]adenine labeling. In experiments with 4-DAMP mustard, cells were washed with 0.5 mL MEM following the 1 hr [^{3}H]adenine labeling and then preincubated with MEM plus 4 μM AF-DX 116 for an additional 15 min at 37° (5% CO_2/95% air). Medium was removed and replaced with 0.5 mL MEM plus 4 μM AF-DX 116 containing either 40 nM activated 4-DAMP mustard or vehicle. Following a 1-hr incubation at 37° in 5% CO_2/95% air, the cells were washed twice with 0.5 mL MEM and used as described above.

2.7. Calculations

The percentages of M_2 and M_3 muscarinic receptors in CHO $M_2 + M_3$ cells were calculated from measurements of the percentage of receptors alkylated by 4-DAMP mustard in CHO M_2, CHO M_3, and CHO $M_2 + M_3$ cells in binding assays using the following calculations. If X denotes the percentage of M_2 receptors and Y the percentage of M_3 receptors in CHO $M_2 + M_3$ cells then:

$$X + Y = 100 \tag{1}$$

It can also be shown that:

$$XA + YB = C \tag{2}$$

where A denotes the percentage of M_2 receptors alkylated by 4-DAMP mustard in CHO M_2 cells, B denotes the percentage of M_3 receptors alkylated in CHO M_3 cells, and C denotes the percentage of receptors alkylated in CHO $M_2 + M_3$ cells. The values of A, B, and C were measured through experimentation, and the values of X and Y were calculated by solving Eqs. (1) and (2) simultaneously. Accordingly, rearrangement of Eq. (1) yields:

$$Y = 100 - X \tag{3}$$

Substitution of Eq. (3) for Y in Eq. (2) followed by rearrangement yields:

$$X = \frac{B - C}{B - A} \times 100 \tag{4}$$

The value of Y can then be estimated from Eq. (3).

The dissociation constant (K_{NMS}) and binding capacity (B_{max}) of [^{3}H]NMS were estimated from the results of experiments in which specific binding was measured at various concentrations of [^{3}H]NMS. Nonlinear regression analysis was used to fit the following equation to the data:

$$y = \frac{[X]B_{max}}{[X] + K_{NMS}} \tag{5}$$

in which y denotes the specific binding of [^{3}H]NMS, and $[X]$ denotes the molar concentration of free [^{3}H]NMS. The binding parameters of AF-DX 116, hexahydrosiladifenidol (HHSiD), and pirenzepine were estimated by measuring the specific binding of [^{3}H]NMS at a fixed concentration in the presence of various concentrations of the nonlabeled muscarinic antagonists. The following one-site competitive binding equation was fitted to the data from CHO M_2 cells using nonlinear regression analysis:

$$y = \frac{P}{1 + (I/K_{d\text{-}M'_2})} \tag{6}$$

in which P denotes the estimate of specific [^{3}H]NMS binding in the absence of the non-labeled antagonist, I denotes the concentration of non-labeled antagonist, and $K_{d\text{-}M'_2}$ denotes the apparent dissociation constant of the non-labeled antagonist for the M_2 receptor. An analogous equation was fitted to the competitive binding data from CHO M_3 cells:

$$y = \frac{P}{1 + (I/K_{d\text{-}M'_3})} \tag{7}$$

In this equation, $K_{d\text{-}M'_3}$ denotes the apparent dissociation constant of the non-labeled antagonist for the M_3 receptor. The following two-site model was fitted to the competitive binding data from CHO $M_2 + M_3$ cells:

$$y = P \times \left(\frac{\alpha'}{1 + (I/K_{d\text{-}M'_2})} + \frac{1 - \alpha'}{1 + (I/K_{d\text{-}M'_3})} \right) \tag{8}$$

In this equation, α' denotes the apparent proportion of M_2 receptors. Eqs. (6)–(8) were fitted to the data both independently and simultaneously. For the simultaneous fit, the estimate of $K_{d\text{-}M'_2}$ was shared between the data from CHO M_2 and CHO $M_2 + M_3$ cells and the estimate of $K_{d\text{-}M'_3}$ was shared between the data from CHO M_3 and CHO $M_2 + M_3$ cells. The apparent dissociation constants (K'_d) of the non-labeled antagonists were corrected for the competitive effect of [^{3}H]NMS using the following equation:

$$K_d = \frac{K'_d}{1 + [[^3\text{H}]\text{NMS}]/K_{NMS}} \tag{9}$$

in which K_d denotes the true dissociation constant of the non-labeled antagonist, [[^{3}H]NMS] denotes the molar concentration of [^{3}H]NMS used in the competition experiment, and K_{NMS} denotes the dissociation constant of [^{3}H]NMS. Different correction factors (i.e. Eq. (9)) were

used for M_2 and M_3 receptors because K_{NMS} was found to differ (approximately 3-fold) between the two receptors. Since the K_{NMS} was not the same for M_2 and M_3 receptors, then receptor occupancy by [^{3}H]NMS at any subsaturating concentration is not the same at the two receptors. Consequently, the apparent proportion of M_2 receptors (α') estimated by regression analysis of the competition curves according to Eq. (8) is not equivalent to the true proportion of M_2 receptors. The apparent proportion of M_2 receptors labeled by [^{3}H]NMS in competition experiments is equal to the amount of M_2 receptors labeled by [^{3}H]NMS divided by the amount of both M_2 and M_3 receptors labeled by [^{3}H]NMS as described by the following equation:

$$\alpha' = \frac{[X]B_{\text{max-M}_2}/([X] + K_{\text{NMS-M}_2})}{([X]B_{\text{max-M}_2}/([X] + K_{\text{NMS-M}_2})) + ([X]B_{\text{max-M}_3}/([X] + K_{\text{NMS-M}_3}))} \quad (10)$$

This equation was derived by calculating receptor occupancy at each receptor according to Eq. (5). The parameters in the above equation are identical to those of Eq. (5) except for the addition of subscripts to discriminate between M_2 and M_3 receptors. Rearrangement of Eq. (10) yields the following equation, which was used to estimate the true proportion of M_2 receptors (α):

$$\alpha = \frac{B_{\text{max-M}_2}}{B_{\text{max-M}_2} + B_{\text{max-M}_3}} = 1 - \frac{1}{1 + (\alpha'([X] + K_{\text{NMS-M}_2})/(1 - \alpha')(X + K_{\text{NMS-M}_3}))} \quad (11)$$

The Hill coefficients (H) of the non-labeled antagonists were estimated by fitting the following equation to the competitive binding data:

$$y = \frac{P}{1 + (I^H/\text{IC}_{50}^H)} \quad (12)$$

In this equation, IC_{50} denotes the concentration of non-labeled antagonist causing a 50% displacement of specific [^{3}H]NMS binding. The IC_{50} values were corrected to yield K_i values (concentration of antagonist yielding 50% receptor occupancy in the absence of [^{3}H]NMS) using an equation analogous to Eq. (9).

The EC_{50} (concentration of agonist causing a half-maximal effect) and E_{max} (maximal effect of the agonist) values of oxotremorine-M for affecting [^{3}H]inositolphosphate and [^{3}H]cAMP accumulation were estimated by fitting an increasing (phosphoinositide hydrolysis) or decreasing (cAMP accumulation) logistic equation to the data as described previously [7]. The dissociation constants (K_b values) of antagonists for antagonizing these functional responses to oxotremorine-M were estimated using the standard competitive inhibition relationship [1]:

$$K_b = \frac{I}{\text{CR} - 1} \quad (13)$$

in which CR (concentration ratio) denotes the EC_{50} value of oxotremorine-M measured in the presence of the antagonist divided by that measured in its absence, and I denotes the concentration of the antagonist. In this analysis, the estimate of E_{max} was shared between the two concentration–response curves. In some experiments on cAMP accumulation in CHO $M_2 + M_3$ cells, the concentration–response curve in the presence of the antagonist exhibited a maximal response a little different from that of the control. In this situation, the CR value was calculated from the control EC_{50} value and the concentration of oxotremorine-M eliciting an equivalent response in the presence of the antagonist.

2.8. Drugs and chemicals

The reagents used in this study were obtained from the following sources: pertussis toxin, List Biological Laboratories, Inc.; DMEM and MEM, Gibco BRL; G 418 sulfate, Omega Scientific; hygromycin-B, CalBiochem; [^{3}H]NMS, [^{3}H]adenine, and [^{3}H]inositol, Dupont New England Nuclear; AF-DX 116, Boehringer Ingelheim Pharmaceutical; HHSiD, pirenzepine, and oxotremorine-M, Research Biochemicals International; atropine, Sigma Chemical Co.; 4-DAMP mustard was synthesized in our laboratory as described previously [6]; and *N*-chloromethylbrucine, Dr. Nigel Birdsall, National Institute for Medical Research. Additional *N*-chloromethylbrucine was synthesized as described by Gharagozloo *et al.* [11].

3. Results

3.1. [^{3}H]NMS binding experiments

CHO cells transfected with a vector containing genes for neomycin resistance and the human M_3 muscarinic receptor (CHO M_3 cells) were transfected a second time with an expression vector containing genes for both the human M_2 muscarinic receptor and resistance to hygromycin. Hygromycin-resistant colonies were selected and screened for the sensitivity of their [^{3}H]NMS binding sites to treatment with 4-DAMP mustard. 4-DAMP mustard is an irreversible muscarinic antagonist that selectively inactivates M_3 receptors over M_2, particularly when receptors are treated with 4-DAMP mustard (40 nM) in the presence of the M_2-selective, competitive antagonist AF-DX 116 (4 μM) for 1 hr [6]. Following this treatment, cell monolayers were washed and assayed for [^{3}H]NMS binding at a concentration of 0.5 nM using a whole cell assay as described under Section 2. Fig. 1 shows the results of [^{3}H]NMS binding assays carried out on intact CHO cells expressing muscarinic receptors. Prior treatment with 4-DAMP mustard only caused a 22% inhibition of [^{3}H]NMS binding to intact CHO M_2 cells. In contrast, 4-DAMP mustard treatment caused 93% inhibition of [^{3}H]NMS binding to CHO M_3

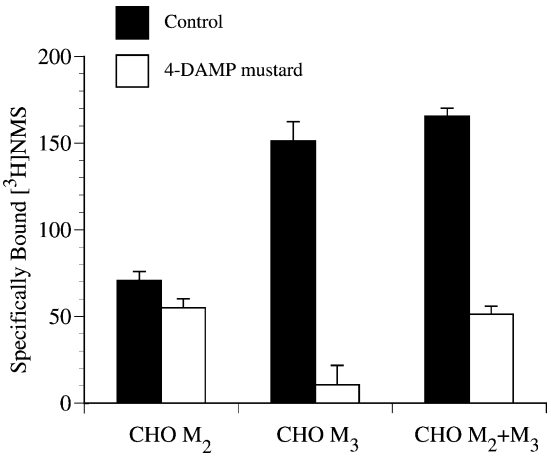

Fig. 1. Specific binding of [^{3}H]NMS in CHO M_2, CHO M_3, and CHO $M_2 + M_3$ cell monolayers before (solid bars) and after (open bars) 4-DAMP mustard treatment. Data represent the mean ± SEM of five experiments for CHO M_2 and CHO M_3 cells and seven experiments for CHO $M_2 + M_3$ cells.

cells. Hygromycin-resistant colonies that had been transfected sequentially with vectors for M_3 and M_2 muscarinic receptors exhibited an intermediate sensitivity (40–80%) to the inhibitory effect of 4-DAMP mustard treatment. Fig. 1 shows binding data from one such colony that served as a source of cells for the remainder of the experiments described in this report. Treatment with 4-DAMP mustard caused a 69% inhibition of [^{3}H]NMS binding in these cells, suggesting that both 4-DAMP mustard-insensitive (M_2) and -sensitive (M_3) muscarinic receptors are expressed in this cell line. In the remainder of the text, we designate these cells as CHO $M_2 + M_3$. By applying Eq. (4) under Section 2 to the data in Fig. 1, we estimated the percentage of M_2 receptors in CHO $M_2 + M_3$ cells to be 34%.

To confirm that the differential effects of 4-DAMP mustard on the binding of [^{3}H]NMS in the three CHO cell lines were due to a decrease in receptor density rather than a change in receptor affinity, the binding of [^{3}H]NMS was measured at various concentrations in cell homogenates before and after treatment with 4-DAMP mustard. Nonlinear regression analysis was used to measure the effect of 4-DAMP mustard on the dissociation constant (K_d) and binding capacity (B_{max}) of [^{3}H]NMS (see Table 1). Treatment with 4-DAMP mustard had little effect on binding affinity as shown by a comparison of K_d values in each cell line. CHO M_2 cells showed no change in K_d values, whereas the K_d values in CHO M_3 and CHO $M_2 + M_3$ cells increased slightly by 1.2- and 1.5-fold, respectively, following 4-DAMP mustard treatment. CHO M_2 cells demonstrated a 3-fold higher K_d for [^{3}H]NMS compared to CHO M_3 cells, consistent with data we have published previously [12]. Compared to the CHO M_2 and CHO M_3 cell lines, CHO $M_2 + M_3$ cells exhibited an intermediate K_d value. The B_{max} values of the three cell lines were differentially affected by 4-DAMP mustard treatment. Whereas the B_{max} in CHO M_2 cell homogenates was hardly affected by 4-DAMP mustard treatment (95% of control value), the B_{max} in CHO M_3 cells was greatly decreased to 3.9% of the control value. The CHO $M_2 + M_3$ cells showed an intermediate B_{max} value (36% of control) following treatment with 4-DAMP mustard. These decreases in B_{max} correspond to 4.8, 96.1, and 64% receptor alkylation in homogenates of CHO M_2, CHO M_3, and CHO $M_2 + M_3$ cells, respectively, in good agreement with the data on intact cells (see Fig. 1; alkylation of 22, 93, and 69% in the same corresponding cell lines). By applying Eq. (4) under Section 2 to the data in Table 1, we estimate the percentage of M_2 receptors in CHO $M_2 + M_3$ cells to be 35%. Total muscarinic receptor density increased upon transfection of CHO M_3 cells with the M_2 gene. Muscarinic receptor density increased from 1.23 ± 0.16 pmol/mg protein in CHO M_3 cells to 1.85 ± 0.32 pmol/mg protein in CHO $M_2 + M_3$ cells as measured by [^{3}H]NMS binding in homogenized extracts of whole cells.

To characterize the pharmacological profile of muscarinic receptors in CHO $M_2 + M_3$ cells, we investigated the binding properties of a series of subtype selective antagonists known to discriminate between M_2 and M_3 muscarinic receptors. For these experiments, the competitive inhibition of [^{3}H]NMS binding at a fixed concentration of 0.5 nM was measured in the presence of increasing concentrations of AF-DX 116, HHSiD, and pirenzepine in the three cell lines (see Fig. 2). We previously measured the pK_i values of AF-DX 116 (6.24, 7.27, 6.10, 6.96, and 5.29), HHSiD (7.66, 6.74, 7.69, 7.65, and 6.77), and pirenzepine (7.77, 5.96, 6.59, 7.23, and 6.55) at M_1, M_2, M_3, M_4, and M_5 receptors, respectively, in CHO cells using the same modified KRB buffer used in this study [13]. The data in Fig. 2 were fitted to a decreasing logistic equation (Eq. (12)) by nonlinear regression analysis to estimate the IC_{50} value and Hill coefficient. The IC_{50} values were

Table 1
Effect of 4-DAMP mustard treatment on the binding parameters of [^{3}H]NMS in CHO cells transfected with M_2 and M_3 muscarinic receptors[a]

	Control		4-DAMP mustard-treated	
	B_{max} (pmol/mg protein)	pK_d	B_{max} (% of control)	pK_d
CHO M_2	2.03 ± 0.75	9.19 ± 0.06	95 ± 16	9.19 ± 0.04
CHO M_3	12.8 ± 1.6	9.68 ± 0.07	3.9 ± 0.19	9.66 ± 0.02
CHO $M_2 + M_3$	10.7 ± 0.03	9.59 ± 0.03	36 ± 8.2	9.41 ± 0.08

[a] Data represent the means ± SEM from three to four experiments, each done in triplicate.

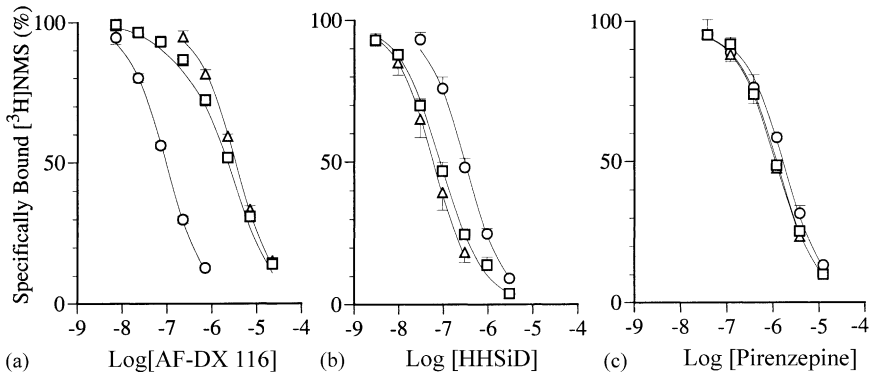

Fig. 2. Competitive inhibition of specifically bound [^{3}H]NMS by AF-DX 116 (a), HHSiD (b), and pirenzepine (c) in CHO cells transfected with M_2 (○), M_3 (△), or both M_2 and M_3 (□) subtypes of the muscarinic receptor. The concentration of [^{3}H]NMS was 0.5 nM. Data are expressed as the percentage of the specific binding of [^{3}H]NMS measured in the absence of antagonist. Each point represents the mean binding value ± SEM of three experiments, each done in triplicate.

corrected for the competitive effect of [^{3}H]NMS to yield the K_i values shown in Table 2. As expected, AF-DX 116 exhibited selectivity for M_2 receptors relative to M_3, whereas the converse was true for HHSiD and pirenzepine. The K_i values generated from competition curves in CHO M_2 and CHO M_3 cells are in good agreement with data we have published previously [13]. In all instances except one, the binding curves of the antagonists yielded very similar Hill coefficients in both the CHO M_2 and CHO M_3 cell lines, indicating behavior consistent with the expression of a single subtype in these cells. The exception was pirenzepine, which exhibited a Hill coefficient of 0.88 in the CHO M_2 cells (see Table 2). We have no adequate explanation for this discrepancy but presume it is related to experimental error. The overall binding affinity of a given antagonist in the CHO $M_2 + M_3$ cells was always intermediate to the affinities observed in M_2 and M_3 cells, but closer to that of the M_3 cell. These results are consistent with a greater expression of M_3 receptors in the CHO $M_2 + M_3$ cell line and with binding affinity at a given receptor being independent of the other receptor. To test this hypothesis, we fitted a two-site model to the competition curves from the CHO $M_2 + M_3$ cells, sharing the estimate of the binding affinity of one site with that of the CHO M_2 cells and the other site with that of the CHO M_3 cells. The results of this analysis yielded antagonist dissociation constants for M_2 and M_3 receptors that are essentially identical to the K_i values listed in Table 2 for CHO M_2 and CHO M_3 cells, respectively. There was no significant improvement in residual error when the competition curves for AF-DX 116 ($F_{2,49} = 1.460$; $P = 0.242$), HHSiD ($F_{2,63} = 0.878$; $P = 0.421$), and pirenzepine ($F_{2,43} = 0.487$; $P = 0.618$) were fitted independently without sharing K_d values between the data from the CHO $M_2 + M_3$ cells and either the CHO M_2 or CHO M_3 cells. In other words, there was no significant difference between the K_d values estimated in CHO $M_2 + M_3$ cells and those estimated in CHO M_2 and CHO M_3 cells. Moreover, the average estimate of the proportion of M_2 receptors in the CHO $M_2 + M_3$ cells was 33% as calculated by nonlinear regression analysis using Eqs. (8) and (11) as described under Section 2. Thus, these results are similar to those observed with 4-DAMP mustard treatment in intact and broken cells where the estimate of M_2 receptors was calculated at 34 and 35%, respectively.

3.2. Phosphoinositide hydrolysis

M_3 muscarinic receptors are known to mediate a stimulation of phosphoinositide hydrolysis in cell lines [14] and in native tissues [15]. Consequently, we investigated the coupling of muscarinic receptors to phosphoinositide hydrolysis in the CHO M_2, CHO M_3, and CHO $M_2 + M_3$ cell lines. The results of these experiments are summarized in Fig. 3 and Table 3. It can be seen that oxotremorine-M, a highly efficacious muscarinic agonist, elicited a robust stimulation of phosphoinositide hydrolysis in the CHO M_3 and CHO $M_3 + M_2$ cells, but not in the

Table 2
Competitive inhibition of [^{3}H]NMS binding by AF-DX 116, HHSiD, and pirenzepine in CHO cells transfected with M_2 and M_3 muscarinic receptors[a]

	AF-DX 116		HHSiD		Pirenzepine	
	pK_i	Hill coefficient	pK_i	Hill coefficient	pK_i	Hill coefficient
CHO M_2	7.30 ± 0.036	0.98 ± 0.012	6.79 ± 0.059	1.01 ± 0.050	6.04 ± 0.049	0.88 ± 0.031
CHO M_3	6.04 ± 0.013	0.94 ± 0.020	7.79 ± 0.124	0.96 ± 0.035	6.51 ± 0.045	0.96 ± 0.064
CHO $M_2 + M_3$	6.15 ± 0.004	0.73 ± 0.049	7.55 ± 0.072	0.85 ± 0.009	6.41 ± 0.028	0.94 ± 0.019

[a] Binding parameters have been estimated from the data shown in Fig. 2. Data represent the means ± SEM from three experiments, each done in triplicate.

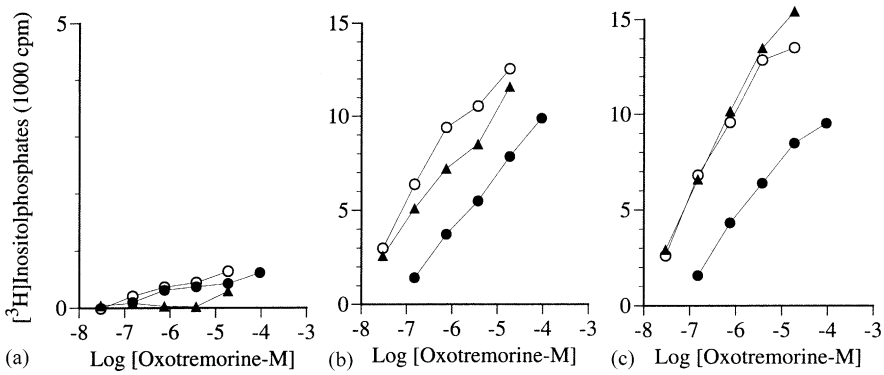

Fig. 3. Effects of 4-DAMP mustard treatment and pertussis toxin treatment on oxotremorine-M-mediated stimulation of phosphoinositide hydrolysis in CHO cells transfected with M_2 (a), M_3 (b), or both M_2 and M_3 (c) muscarinic receptors. Oxotremorine-M-stimulated phosphoinositide hydrolysis was measured in control cells (○), in cells incubated with pertussis toxin (0.1 μg/mL) for 16–18 hr (▲) and in cells treated with 4-DAMP mustard (40 nM) in combination with AF-DX 116 (4.0 μM) for 1 hr (●). The data of one representative experiment from a total of two are shown.

CHO M_2 cells. Overnight treatment with pertussis toxin had little effect on phosphoinositide hydrolysis in the M_3 receptor expressing cells, but greatly inhibited the weak phosphoinositide response observed in the CHO M_2 cell line. Prior treatment of the cells for 1 hr with 4-DAMP mustard (40 nM) in combination with AF-DX 116 (4.0 μM) followed by washing caused a subsequent, large inhibition of oxotremorine-M-mediated phosphoinositide hydrolysis in the M_3 receptor expressing cells, but had little effect in the CHO M_2 cell line. An additional experiment utilizing a longer incubation (2-hr) with 4-DAMP mustard yielded similar results. These data are consistent with the postulate that the phosphoinositide response is mediated primarily by the 4-DAMP mustard-sensitive M_3 receptor via the pertussis toxin-insensitive G protein, G_q.

To characterize the pharmacological profile of the muscarinic phosphoinositide response in the CHO M_3 and CHO $M_2 + M_3$ cells, we measured the potency with which AF-DX 116, HHSiD, and pirenzepine, subtype selective antagonists, interfered with the response. In these experiments, oxotremorine-M-mediated phosphoinositide hydrolysis was measured in CHO M_3 (Fig. 4a) and CHO $M_2 + M_3$ cells (Fig. 4b) in the presence and absence of a single concentration of either AF-DX 116, pirenzepine, or HHSiD. For the experiments shown in Fig. 4a and b, cells were prelabeled overnight with [^{3}H]inositol before agonist-mediated phosphoinositide hydrolysis was measured. Antagonist dissociation constants (K_b values) were estimated from the magnitude of the rightward shift of the oxotremorine-M concentration–response curve caused by each antagonist as described under Section 2, and the negative logarithms of these values (pK_b) are listed in Table 4. The pK_b values of the antagonists were similar in both the CHO M_3 and CHO $M_2 + M_3$ cells, indicating that the M_3 receptor is primarily responsible for eliciting the response in the two cell lines. There was good agreement between the pK_b values of AF-DX 116 and HHSiD for antagonizing the phosphoinositide response and their respective binding affinities at M_3 muscarinic receptors (see Table 2). In contrast, the pK_b values of pirenzepine in both the CHO M_3 and CHO $M_2 + M_3$ cells were approximately one log unit greater than the binding affinity measured at the M_3 receptor (see Table 2). Thus, pirenzepine appeared to exhibit an apparent 10-fold greater potency in the functional assay as compared to the binding assay.

Pirenzepine has been shown to equilibrate slowly with muscarinic receptors [16]. It is possible that the discrepancy between binding affinity and functional antagonism is due to incomplete equilibration of the agonist with the

Table 3
Activity of oxotremorine-M in second messenger assays in CHO cells transfected with M_2 and M_3 muscarinic receptors[a]

	Phosphoinositide hydrolysis		cAMP accumulation	
	pEC_{50}[b]	E_{max}[c] (cpm)	pEC_{50}[b]	E_{max}[d] (% inhibition)
CHO M_2	5.08 ± 0.17	840 ± 130	7.08 ± 0.05	61 ± 1.7
CHO M_3	6.01 ± 0.09	95000 ± 8200	6.25 ± 0.32	29 ± 3.0
CHO $M_2 + M_3$	6.23 ± 0.09	72000 ± 1900	7.44 ± 0.17	85 ± 2.8

[a] Pharmacological parameters have been estimated from the data in Figs. 3, 4, 6, and 7. Data represent the means ± SEM from two to four experiments, each done in triplicate.

[b] Denotes the negative logarithm of the EC_{50} value of oxotremorine-M.

[c] Denotes the maximal stimulatory effect of oxotremorine-M on phosphoinositide hydrolysis.

[d] Denotes the maximal inhibitory effect of oxotremorine-M on cAMP accumulation. In CHO cells expressing M_3 muscarinic receptors, rebound stimulation in cAMP accumulation occurred at oxotremorine-M concentrations greater than that which elicited the maximal inhibitory effect.

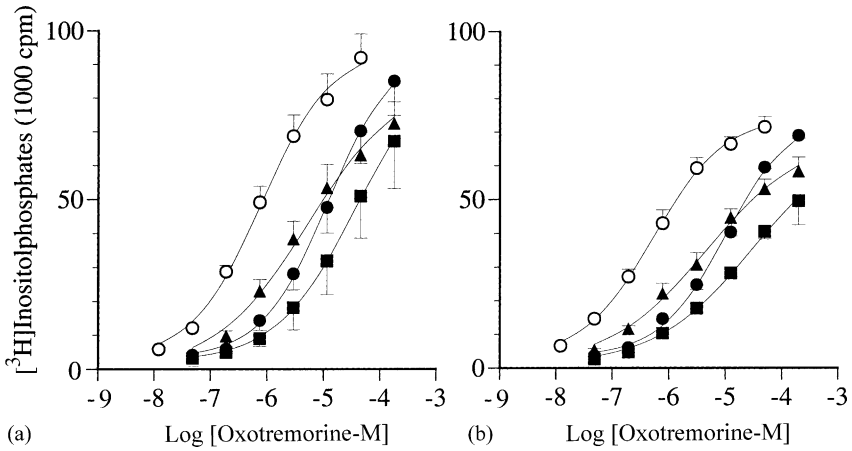

Fig. 4. Stimulation of phosphoinositide hydrolysis by oxotremorine-M in CHO cells transfected with M_3 (a), or both M_2 and M_3 (b) muscarinic receptors in the absence and presence of selective muscarinic antagonists. Oxotremorine-M-stimulated phosphoinositide hydrolysis was measured in the absence (○) or presence of 8.74 μM AF-DX 116 (●), 0.225 μM HHSiD (▲), or 2.80 μM pirenzepine (■). Each data point represents the mean ± SEM of three experiments, each done in triplicate.

M_3 receptor under the conditions of the assay. This situation might be expected because the cells are first labeled with [^{3}H]inositol and pre-equilibrated with the antagonist before addition of the agonist. As soon as the agonist is added, a measurable accumulation of [^{3}H]inositolphosphates occurs. If pirenzepine dissociates slowly from the muscarinic receptor, then the agonist will be unable to compete it off the receptor rapidly, and the amount of [^{3}H]inositolphosphates accumulated during the assay will be lower than that expected at equilibrium. To avoid this potential problem, cells were allowed to come to equilibrium with a single concentration of pirenzepine in combination with the various concentrations of oxotremorine-M for 30 min. Then the [^{3}H]inositol was added, and the incubation was allowed to continue for another 45 min. It can be seen in Fig. 5a and b, that the pirenzepine-induced shifts in the oxotremorine-M concentration–response curves are less when measured using the continuous labeling paradigm as compared with those measured using the prelabeling method. Moreover, when [^{3}H]inositolphosphate accumulation was measured using the continuous labeling technique, the K_b values of pirenzepine in CHO $M_2 + M_3$ cells (0.20 μM) and CHO M_3 cells (0.091 μM) more closely approximated the K_i value for binding to muscarinic receptors expressed in CHO M_3 cells (0.33 μM). Table 4 also lists the pK_b values of pirenzepine measured using the continuous labeling paradigm.

3.3. cAMP accumulation

M_2 muscarinic receptors are known to mediate an inhibition of cAMP accumulation in cell lines and in native tissues. Consequently, we investigated the coupling of muscarinic receptors to adenylyl cyclase in the CHO M_2, CHO M_3, and CHO $M_2 + M_3$ cell lines (see Fig. 6a and Table 3). By itself, forskolin stimulated cAMP accumulation in intact CHO M_3 cells an average of 22-fold over basal, significantly higher than the 16-fold increase observed in CHO $M_2 + M_3$ cells. The cAMP accumulation in CHO M_2 cells was elevated 12-fold by forskolin treatment. Oxotremorine-M caused a maximal inhibition of forskolin-stimulated cAMP production in CHO M_2 cells of 55% with an EC_{50} value of 0.02 μM. Maximal inhibition was achieved at a concentration of 0.2 μM oxotremorine-M;

Table 4
Antagonism of the phosphoinositide response to oxotremorine-M in CHO cells transfected with M_2 and M_3 muscarinic receptors[a]

	CHO M_3		CHO $M_2 + M_3$		Binding affinity (pK_d)	
	Shift[b]	pK_b	Shift[b]	pK_b	CHO M_2	CHO M_3
AF-DX 116 (8.74 μM)	15.6 (1.19 ± 0.15)	6.22 ± 0.16	17.5 (1.24 ± 0.07)	6.28 ± 0.08	7.30 ± 0.036	6.04 ± 0.013
HHSiD (0.225 μM)	13.3 (1.12 ± 0.10)	7.74 ± 0.11	14.8 (1.17 ± 0.07)	7.79 ± 0.08	6.79 ± 0.059	7.79 ± 0.12
Pirenzepine (2.8 μM)	68 (1.83 ± 0.13)	7.38 ± 0.13	95 (1.98 ± 0.17)	7.52 ± 0.17	6.04 ± 0.049	6.51 ± 0.045
	32[c] (1.50 ± 0.05)	7.04 ± 0.05[c]	14.7[c] (1.17 ± 0.07)	6.69 ± 0.07[c]		

[a] Pharmacological parameters have been estimated from the data for phosphoinositide hydrolysis shown in Figs. 4 and 5 and the binding data shown in Fig. 2. Unless indicated otherwise, phosphoinositide hydrolysis was measured using the prelabeling technique described under Section 2. Data represent the means ± SEM from three experiments, each done in triplicate.

[b] Denotes the EC_{50} value of oxotremorine-M measured in the presence of the antagonist divided by that measured in its absence. The log shift values ± SEM are denoted in parentheses beneath each shift value.

[c] Phosphoinositide hydrolysis was measured using the continuous labeling technique as described under Section 2.

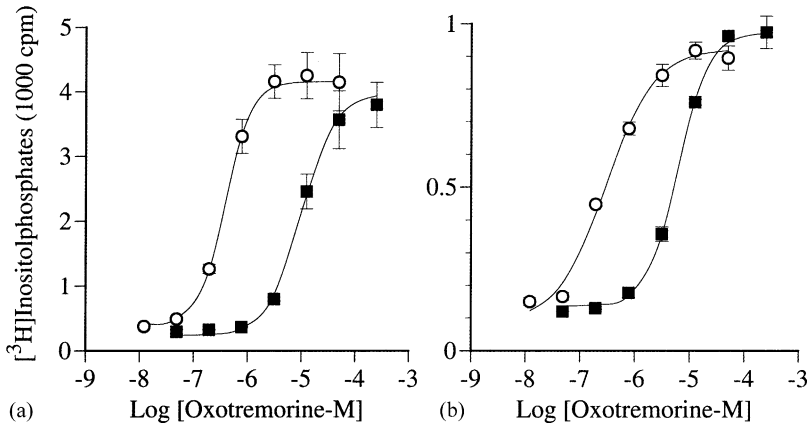

Fig. 5. Stimulation of phosphoinositide hydrolysis by oxotremorine-M in CHO cells transfected with M_3 (a), or both M_2 and M_3 (b) muscarinic receptors using a continuous [^{3}H]inositol labeling paradigm. CHO cells were incubated with various concentrations of oxotremorine-M in the absence (○) or presence (■) of 2.80 μM pirenzepine. After 30 min at 37°, [^{3}H]inositol was added to each well, and the incubation was continued for an additional 45 min, after which total [^{3}H]inositolphosphates were measured. Each data point represents the mean ± SEM of three experiments, each done in triplicate.

higher concentrations elicited no additional response. Oxotremorine-M demonstrated a similar maximal inhibition of cAMP production in CHO $M_2 + M_3$ cells of 52%, although inhibitions as great as 80% were seen in individual experiments (CHO M_2 cells never showed inhibition greater than 60%). Oxotremorine-M was slightly less potent in CHO $M_2 + M_3$ cells having an EC_{50} of 0.07 μM. At higher concentrations of oxotremorine-M (>1 μM), the inhibition of cAMP production was reversed in CHO $M_2 + M_3$ cells, and at the highest concentration of oxotremorine-M tested (200 μM), cAMP production was actually 1.3-fold greater than forskolin-stimulated control levels. Unexpectedly, oxotremorine-M was also able to inhibit cAMP production in CHO M_3 cells although to a lesser extent (23% maximal inhibition) and with a less potent EC_{50} (0.5 μM). Higher concentrations of oxotremorine-M resulted in the same rebound increase in cAMP accumulation as seen in CHO $M_2 + M_3$ cells with cAMP levels starting to increase at concentrations greater than 2 μM oxotremorine-M and returning to those of the forskolin-stimulated control at a concentration of 200 μM oxotremorine-M. CHO M_2 cells displayed a very slight increase in cAMP accumulation at high oxotremorine-M concentrations relative to the maximal inhibition observed at 0.2 μM.

It is known that the M_2 muscarinic receptor mediates an inhibition of adenylyl cyclase through G_i. To verify that the inhibition of cAMP production in CHO $M_2 + M_3$ cells was mediated by G_i, cultured cells were treated with pertussis toxin to uncouple G_i from M_2 receptors. Oxotremorine-M inhibition of forskolin-stimulated cAMP production in each of the CHO cell lines following pertussis toxin treatment is illustrated in Fig. 6b. Overnight pertussis toxin treatment inhibited forskolin-stimulated cAMP production by 60% in each CHO cell line and eliminated the oxotremorine-M-mediated inhibition of cAMP accumulation. At higher concentrations of oxotremorine-M, treatment with pertussis toxin unmasked a marked stimulation of cAMP production in each CHO cell line. At a concentration of 200 μM, oxotremorine-M stimulated cAMP production 4.3-, 3.0-, and 2.2-fold in the CHO $M_2 + M_3$, CHO M_3, and CHO M_2 cell lines, respectively. The stimulation of cAMP production occurred over the same concentration

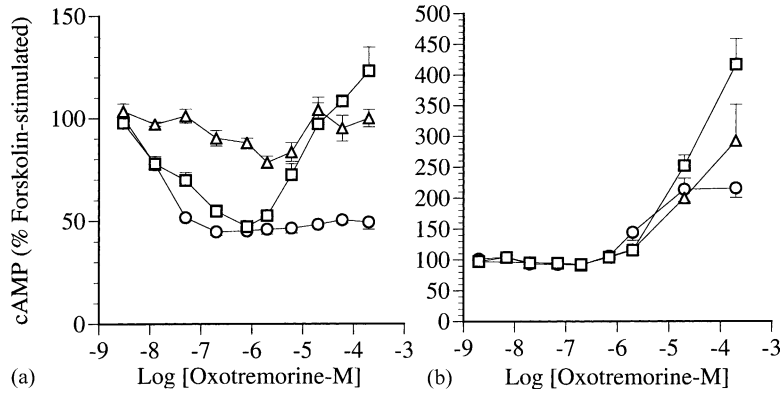

Fig. 6. Effects of various concentrations of oxotremorine-M on forskolin-stimulated cAMP accumulation in CHO cells before (a) and after (b) pertussis toxin treatment. Forskolin (10 μM) stimulated cAMP accumulation was measured in CHO cells transfected with the M_2 (○), M_3 (△), or both M_2 and M_3 (□) subtypes of the muscarinic receptor. Data are expressed as the percentage of forskolin-stimulated cAMP accumulation measured in the absence of oxotremorine-M. Each data point represents the mean ± SEM of at least three experiments.

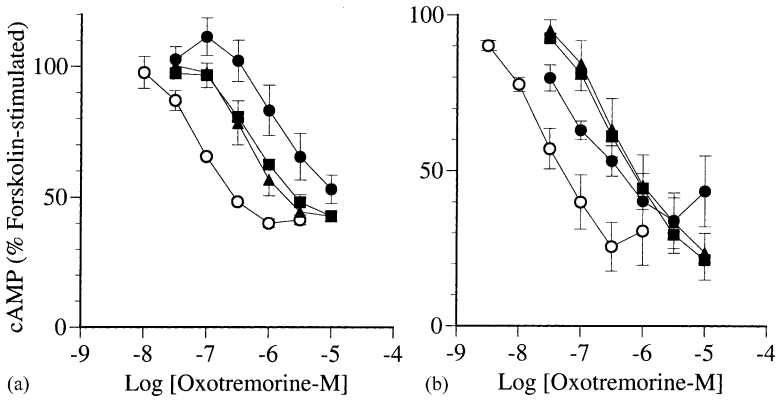

Fig. 7. Effect of selective muscarinic receptor antagonists on the inhibition of forskolin-stimulated cAMP accumulation by oxotremorine-M in CHO cells transfected with M_2 (a) or both M_2 and M_3 (b) muscarinic receptors. Oxotremorine-M-mediated inhibition of cAMP accumulation was measured in the absence (○) and presence of 0.59 μM AF-DX 116 (●), 2.0 μM HHSiD (▲), or 12 μM pirenzepine (■). The concentration of forskolin was 10 μM. Data are expressed as the percentage of forskolin-stimulated cAMP accumulation measured in the absence of oxotremorine-M. Each data point represents the mean ± SEM of three experiments, each done in triplicate.

range of oxotremorine-M as seen in control cells not treated with pertussis toxin.

To characterize the pharmacological profile of the muscarinic cAMP response in the CHO M_2 and CHO $M_2 + M_3$ cells, we measured the potency with which the subtype selective antagonists AF-DX 116, HHSiD, and pirenzepine interfered with the response. In these experiments, oxotremorine-M-mediated inhibition of forskolin-stimulated cAMP accumulation was measured in CHO M_2 (Fig. 7a) and CHO $M_2 + M_3$ (Fig. 7b) cells in the presence and absence of a single concentration of either AF-DX 116, HHSiD, or pirenzepine. Antagonist dissociation constants (K_b values) were estimated from the magnitude of the rightward shift of the oxotremorine-M concentration–response curve caused by each antagonist as described under Section 2, and the negative logarithms of these values are listed in Table 5. In the CHO M_2 cells, oxotremorine-M caused a maximal 61% inhibition of cAMP accumulation with the EC_{50} value for this effect being 0.093 μM. AF-DX 116 (0.59 μM), HHSiD (2.0 μM), and pirenzepine (12 μM) shifted the concentration–response curve of oxotremorine-M to the right in a parallel fashion without significantly affecting the maximal response. Moreover, the estimates of the pK_b values of the antagonists are in general agreement with the binding affinities of the same antagonists for the M_2 receptor. In the CHO $M_2 + M_3$ cells, the shift in the oxotremorine-M concentration–response curve caused by AF-DX 116 was approximately one-third that observed in the CHO M_2 cells, whereas the converse was observed for HHSiD and pirenzepine. The shifts caused by these antagonists in the CHO $M_2 + M_3$ cells were more than 2-fold greater than those observed in the CHO M_2 cells.

It is possible that the differences between the antagonism of the muscarinic cAMP response in the CHO M_2 and the CHO $M_2 + M_3$ cells is due to the contribution of the M_3 receptor to the response in the latter cells. Our prior data in CHO M_3 cells showed that M_3 receptors were able to mediate a productive inhibition of cAMP accumulation (although not as effective as the M_2 receptor; see Fig. 6a). One might expect, therefore, that the pharmacological antagonism of this response in the CHO $M_2 + M_3$ cells might exhibit properties in between M_2- and M_3-like. To test this postulate, we measured the effect of AF-DX 116 on oxotremorine-M-mediated inhibition of forskolin-stimulated cAMP accumulation in CHO $M_2 + M_3$ cells, before and after treatment with 4-DAMP mustard. 4-DAMP mustard treatment should inactivate most of the M_3 receptors. We also ran similar control experiments with CHO M_2 cells to determine the effect, if any, of 4-DAMP

Table 5
Antagonism of oxotremorine-M-mediated inhibition of forskolin-stimulated cAMP accumulation in CHO cells transfected with M_2 and M_3 muscarinic receptors[a]

	CHO M_2		CHO $M_2 + M_3$		Binding affinity (pK_d)	
	Shift[b]	pK_b	Shift[b]	pK_b	CHO M_2	CHO M_3
AF-DX 116 (0.59 μM)	24 (1.38 ± 0.23)	7.59 ± 0.24	8.1 (0.91 ± 0.06)	7.08 ± 0.07	7.30 ± 0.036	6.04 ± 0.013
HHSiD (2.0 μM)	5.2 (0.72 ± 0.16)	6.30 ± 0.22	12.8 (1.11 ± 0.13)	6.77 ± 0.15	6.79 ± 0.059	7.79 ± 0.12
Pirenzepine (12 μM)	6.0 (0.78 ± 0.04)	5.62 ± 0.05	12.0 (1.08 ± 0.02)	5.97 ± 0.02	6.04 ± 0.049	6.51 ± 0.045

[a] Pharmacological parameters have been estimated from the data for cAMP accumulation shown in Fig. 7 and the binding data shown in Fig. 2. Data represent the means ± SEM from three experiments, each done in triplicate.

[b] Denotes the EC_{50} value of oxotremorine-M measured in the presence of the antagonist divided by that measured in its absence. The log shift values ± SEM are denoted in parentheses beneath each shift value.

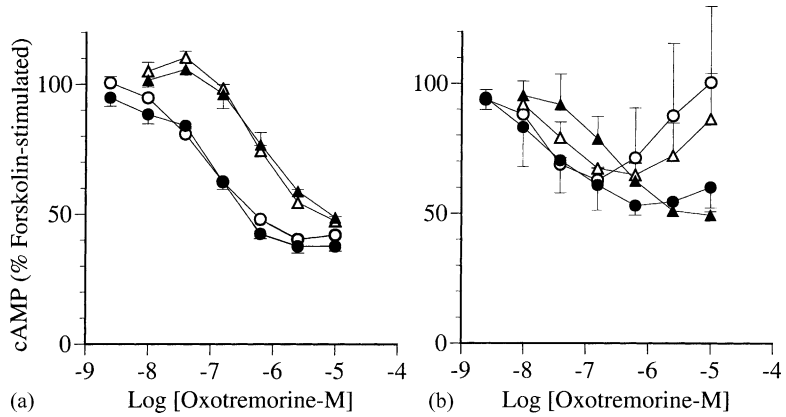

Fig. 8. Effects of AF-DX 116 and prior treatment with 4-DAMP mustard on oxotremorine-M-mediated inhibition of forskolin-stimulated cAMP accumulation in CHO cells transfected with either M_2 (a) or both M_2 and M_3 (b) muscarinic receptors. 4-DAMP mustard treatment was accomplished by incubating cells with the cyclized mustard (40 nM) in combination with AF-DX 116 (4 μM) for 1 hr at 37° followed by extensive washing. Control cells were treated similarly except for exposure to 4-DAMP mustard. Forskolin-stimulated cAMP accumulation was measured in control (○, △) and 4-DAMP mustard-treated cells (●, ▲) in the absence (○, ●) and presence (△, ▲) of 0.59 μM AF-DX 116. The concentration of forskolin was 10 μM. The data are expressed as the percentage of forskolin-stimulated cAMP accumulation measured in the absence of oxotremorine-M. Each data point represents the mean ± SEM of three experiments, each done in triplicate.

mustard on the M_2 cAMP response. Fig. 8a shows that AF-DX 116 caused a parallel, 7.3-fold rightward shift in the oxotremorine-M concentration–response curve in CHO M_2 cells and that 4-DAMP mustard treatment had no significant influence on the effect of AF-DX 116. These results are consistent with our prior binding data showing that 4-DAMP mustard has little or no effect on M_2 receptors. In contrast, treatment with 4-DAMP mustard enhanced the potency of AF-DX 116 for antagonizing oxotremorine-M-mediated inhibition of cAMP accumulation in the CHO $M_2 + M_3$ cells (see Fig. 8b). The shift in the concentration–response curve caused by AF-DX 116 increased from 2.5-fold in the control to 4.8-fold following 4-DAMP mustard treatment of the CHO $M_2 + M_3$ cells.

We also investigated the effects of *N*-chloromethylbrucine, a novel allosteric agent, on oxotremorine-M-mediated changes in cAMP accumulation in CHO M_2, CHO M_3, and CHO $M_2 + M_3$ cells (Fig. 9). *N*-Chloromethylbrucine is a novel allosteric agent first described by Birdsall *et al.* [17] that tunes up the responses of acetylcholine at M_3 receptors and inhibits responses at M_2 receptors. We also found that *N*-chloromethylbrucine (0.2 mM) shifted the oxotremorine-M concentration–response curve for inhibition of cAMP accumulation in CHO M_2 cells to the right about 2-fold (Fig. 9a). In contrast, the same concentration of *N*-chloromethylbrucine shifted the concentration–response curve of oxotremorine-M to the left in CHO M_3 cells about 4-fold (Fig. 9b). In the CHO $M_2 + M_3$ cells, *N*-chloromethylbrucine had little or no effect on the oxotremorine-M concentration–response curve (Fig. 9c).

4. Discussion

Our experiments with 4-DAMP mustard show that this irreversible antagonist is a useful probe for discriminating between M_2 and M_3 muscarinic receptors. When receptors were first incubated with 4-DAMP mustard (40 nM) in the presence of the competitive, M_2 selective antagonist AF-DX 116 (4 μM) for 1 hr and then washed extensively, we

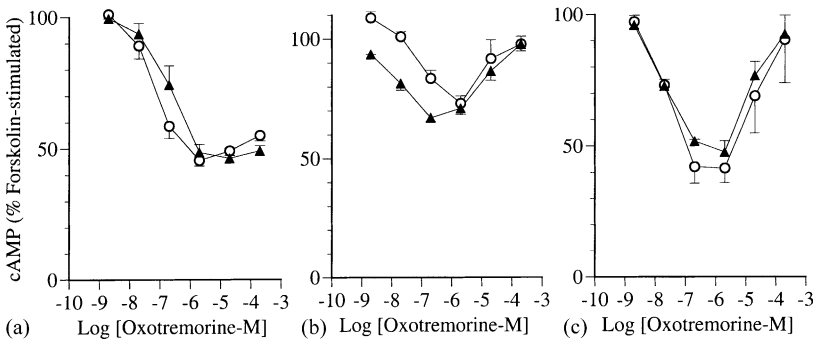

Fig. 9. Effect of *N*-chloromethylbrucine on oxotremorine-M-mediated inhibition of forskolin-stimulated cAMP accumulation in CHO cells transfected with M_2 (a), M_3 (b), or both M_2 and M_3 (c) subtypes of the muscarinic receptors. The accumulation of cAMP was measured in the absence (○) and presence (▲) of 200 μM *N*-chloromethylbrucine. The concentration of forskolin was 10 μM. The data are expressed as the percentage of forskolin-stimulated cAMP accumulation measured in the absence of oxotremorine-M. Each point represents the mean ± SEM of three experiments, each done in triplicate.

noted an approximately 95% inhibition of [^{3}H]NMS binding to M_3 receptors and only a 5–20% inhibition at M_2 receptors. The reduction in binding was associated with a decrease in B_{max} without an effect on affinity, which is consistent with the postulate that the mustard causes an irreversible alkylation of the binding site on muscarinic receptors. We have noted similar results in work on native tissues [6].

In our experiments on oxotremorine-M-mediated phosphoinositide hydrolysis, we noted good agreement between the potency of antagonists for blocking phosphoinositide hydrolysis in the CHO M_3 and CHO $M_2 + M_3$ cells and their respective binding affinities at the M_3 receptor. Initially, we noted a discrepancy with regard to pirenzepine. However, this situation could be attributed to a lack of equilibrium between pirenzepine and oxotremorine-M. When pirenzepine and oxotremorine-M were first allowed to reach equilibrium before the addition of the [^{3}H]inositol, we found good agreement between binding affinity and functional antagonism. Thus, our results are consistent with the postulate that it is primarily the M_3 receptor that triggers phosphoinositide hydrolysis in the CHO $M_2 + M_3$ cells and that there is little contribution of the M_2 receptor. Accordingly, we noted that the phosphoinositide response to oxotremorine-M was very small in the CHO M_2 cells. This small response was pertussis toxin-sensitive, unlike the phosphoinositide response in CHO M_3 and CHO $M_2 + M_3$ cells, which was insensitive to pertussis toxin. Thus, G_i or G_o probably mediates the response in CHO M_2 cells, whereas G_q is likely to mediate the response in the M_3 receptor expressing cells. We also noted that the phosphoinositide responses in CHO M_3 and CHO $M_2 + M_3$ cells were inhibited equally by treatment with 4-DAMP mustard, further suggesting that it is primarily the M_3 receptor that mediates the response in these cells.

The expression of M_2 muscarinic receptors in CHO $M_2 + M_3$ cells was also confirmed in functional assays that demonstrated an oxotremorine-M-mediated inhibition of forskolin-stimulated cAMP production. Unexpectedly, we observed a muscarinic agonist-mediated inhibition of forskolin-stimulated cAMP accumulation in CHO M_3 cells. However, this effect was weak and displayed a relatively low potency ($EC_{50} = 0.50\ \mu M$) and maximal response ($E_{max} = 23\%$ inhibition). Transfection of the M_2 receptor into the M_3 cell line resulted in a more robust oxotremorine-M-mediated inhibition of cAMP accumulation characterized by a more potent EC_{50} value and a greater maximal inhibition (50–80%). The magnitude of the inhibitory phase of the concentration–response curve for oxotremorine-M in the CHO $M_2 + M_3$ cells was comparable to that observed in the CHO M_2 cells. The inhibitory phase of the oxotremorine-M concentration–response curve in the CHO M_3 cells, like that of the CHO M_2 and CHO $M_2 + M_3$ cells, was inhibited by pertussis toxin, indicating that G_i is involved in mediating this response in the three cell lines.

The inhibitory effect of oxotremorine-M on cAMP levels in CHO M_3 and CHO $M_2 + M_3$ cells was reversed at high concentrations where stimulation in cAMP accumulation was observed. In contrast, this stimulatory phase was not observed in the CHO M_2 cells, suggesting that the stimulation is mediated primarily by the M_3 receptor in the CHO $M_2 + M_3$ cells. Treatment with pertussis toxin eliminated the high potency, agonist-mediated inhibition of cAMP accumulation and enhanced the low potency stimulation of cAMP accumulation in the three cell lines. Thus, following pertussis toxin treatment, the CHO M_2 cells exhibited an agonist-mediated stimulation of cAMP accumulation. These results suggest that both M_2 and M_3 receptors can couple with G_s, although the robust M_2 receptor-mediated inhibition of cAMP accumulation obscures the lower potency, stimulatory mechanism in CHO M_2 cells. Other investigators have noticed that M_2 receptors mediate a stimulation of cAMP accumulation in CHO cells in the absence of pertussis toxin and that this effect is dependent upon the incubation time and is more apparent with high expression of M_2 receptors [18].

The mechanism for the stimulation in cAMP accumulation mediated through M_2 and M_3 receptors at high levels of agonist occupancy is unclear. We noted a small stimulation in cAMP accumulation (2.5-fold increase over basal) by a high concentration of oxotremorine-M (i.e. 10–100 μM) in M_3 CHO cells in the absence of forskolin (data not shown), suggesting that the M_3 receptor weakly couples to $G_{\alpha s}$ to stimulate adenylyl cyclase. Forskolin is known to enhance the stimulatory effect of $G_{\alpha s}$ at many subtypes of adenylyl cyclase [19–21], which can explain why the muscarinic receptor-mediated increase in cAMP accumulation is greater in the presence of forskolin. Another possible mechanism could involve the significant expression of type II and IV adenylyl cyclases in CHO cells, which are known to be stimulated by $G_{\beta\gamma}$ [19,22]. The source of $G_{\beta\gamma}$ could be M_3 receptor-mediated activation of G_q. However, this stimulation is conditional upon activation by $G_{\alpha s}$, and thus this hypothesis also depends upon direct M_3 receptor activation of G_s. Also, we are unaware of reports demonstrating the expression of type II and IV cyclase in CHO cells. M_2 muscarinic receptors were shown to mediate a stimulation in cAMP accumulation in pertussis toxin-treated CHO cells. However, it seems unlikely that this mechanism involves the liberation of $G_{\beta\gamma}$ from G_q because M_2 receptor activation had little or no effect on phosphoinositide hydrolysis after pertussis toxin treatment (see Fig. 3a as well as Ashkenazi *et al.* [23]). Consequently, we think that the most likely explanation for the muscarinic stimulation of cAMP accumulation is a direct coupling of M_2 and M_3 receptors to G_s.

The competitive antagonism of the cAMP response in CHO M_2 cells was relatively straightforward. The antagonists shifted the oxotremorine-M concentration–response curve to the right in a parallel fashion without significantly affecting the maximal response. Moreover, the dissociation

constants of the antagonists, measured by pharmacological antagonism (K_b values), were in good agreement with those estimated in competitive binding assays with [^{3}H]NMS. In contrast, the competitive antagonism of the response in CHO $M_2 + M_3$ cells was more complex. In the presence of AF-DX 116, the potent inhibitory phase of the concentration–response curve exhibited less of a maximal response compared to control, whereas the converse was observed in the presence of pirenzepine or HHSiD. These results can be explained by the M_2–M_3 selectivity of the antagonists and the greater contribution of the M_3 receptor to the low potency, stimulatory phase of the concentration–response curve. AF-DX 116 is an M_2 selective antagonist and would therefore be expected to interfere more effectively with the more potent, M_2 inhibitory phase of the concentration–response curve than the less potent, M_3 stimulatory phase of the curve. Since the maximal inhibition of cAMP accumulation in the CHO $M_2 + M_3$ cells probably represents a balance between M_2 inhibitory and M_3 stimulatory effects, a decrease in the maximal inhibition would be expected in the presence of AF-DX 116. In contrast, the opposite would be expected in the presence of HHSiD or pirenzepine since these latter agents exhibit selectivity for M_3 receptors relative to M_2. As described above, this type of behavior was observed.

Since the subtype selective muscarinic antagonists caused changes in the maximal inhibitory response to oxotremorine-M in the CHO $M_2 + M_3$ cells, we measured the antagonist-induced shift based on an absolute level of inhibition of cAMP accumulation as described under Section 2. Using this approach, we noted that the potency of AF-DX 116 for antagonizing oxotremorine-M-mediated inhibition of cAMP accumulation in CHO $M_2 + M_3$ cells was approximately 2-fold less than that observed in CHO M_2 cells, whereas the converse was true for HHSiD and pirenzepine. These results can be rationalized by the contribution of both M_2 and M_3 receptors to the inhibitory phase of the concentration–response curve (see Fig. 6) and to the M_2–M_3 selectivity of the antagonists. Since AF-DX 116 is M_2 selective, its potency for antagonizing a combined M_2–M_3 response should be less than that expected for a pure M_2 response. Conversely, since HHSiD and pirenzepine exhibit selectivity for M_3 receptors over M_2, their potency for antagonizing a combined M_2–M_3 response should be greater than that expected for a pure M_2 response. Thus, our data are consistent with the postulate that both M_2 and M_3 receptors mediate an inhibition of cAMP accumulation in the CHO $M_2 + M_3$ cells, although the M_2 receptor appears to have a larger role. This hypothesis is consistent with our observation that inactivation of M_3 receptors in the CHO $M_2 + M_3$ cells with 4-DAMP mustard increased the antagonist potency of AF-DX 116 similar to that observed in CHO M_2 cells.

Our experiments with the novel allosteric modulator of muscarinic receptors, *N*-chloromethylbrucine, are consistent with the latter hypothesis. Birdsall *et al.* [17] have shown that *N*-chloromethylbrucine interacts allosterically with muscarinic receptors to enhance the response to acetylcholine at M_3 receptors and to inhibit its action at M_2 receptors. These reciprocal changes in function can be attributed to corresponding allosteric effects on acetylcholine binding affinity at M_2 and M_3 receptors [24]. We report similar observations here using oxotremorine-M as the agonist and the cAMP assay as a measure of function. Interpolation of the data reported by Birdsall *et al.* [17] on [^{35}S]GTPγS binding in CHO cells predicts that *N*-chloromethylbrucine would enhance the potency of acetylcholine at M_3 receptors about 4-fold when present at 0.2 mM, whereas the same concentration of *N*-chloromethylbrucine would reduce the potency of acetylcholine at M_2 receptors to about one-fourth. In our studies with *N*-chloromethylbrucine (0.2 mM), we observed a similar effect on the potency of oxotremorine-M at M_3 receptors but a smaller effect at M_2 receptors (i.e. potency reduced to one-half). This modest difference might be due to the use of oxotremorine-M in our studies. It is known that allosteric agents have different effects, depending upon the ligand with which they are interacting. In contrast, *N*-chloromethylbrucine had little effect on oxotremorine-M-mediated inhibition of cAMP accumulation in CHO $M_2 + M_3$ cells. These results are consistent with the idea that both M_2 and M_3 receptors contribute to the response in these cells, since the opposing effects of *N*-chloromethylbrucine on these two receptors would be expected to cancel out.

Recombinant, chimeric proteins provide a unique perspective for investigating receptor–receptor interactions between G protein-coupled receptors. Maggio *et al.* [25] and Barbier *et al.* [26] have co-expressed truncated, wild-type, and point mutants of M_2 and M_3 muscarinic receptors in COS-7 cells, and have carried out binding studies on membranes prepared from these cells. Their data suggest that wild-type M_2 and M_3 receptors may undergo amino terminal and carboxy terminal domain exchange to yield a receptor with unique pharmacological properties when transiently expressed in COS-7 cells. It was suggested that oligomerization of M_2 and M_3 receptors results in the association of the amino terminal portion of the M_2 receptor with the carboxy terminal portion of the M_3 receptor to yield a pharmacologically distinct binding site, characterized by its high affinity for pirenzepine. Although no direct measure of the affinity of pirenzepine for an oligomeric M_2/M_3 muscarinic receptor was made, a pK_d value of approximately 7.5 was estimated on the basis of its affinity for muscarinic sites labeled with [^{3}H]NMS in COS-7 cells expressing fragments of both M_2 (M_2 trunc) and M_3 (M_3 tail) receptors. This estimate of binding affinity is approximately 10- and 30-fold greater than those of pirenzepine for M_3 and M_2 receptors, respectively (see Table 2). Our results with wild-type M_2 and M_3 muscarinic receptors provide no evidence for the presence of a heteromeric complex with high affinity for pirenzepine. It is

conceivable that such a complex exists, but is in too low abundance for us to detect in our binding and functional assays.

We have described the construction of a CHO cell that expresses both the M_2 and M_3 muscarinic receptor subtypes and have characterized the receptor population pharmacologically. The binding and functional data are consistent with those expected if the receptor subtypes act independently of one another without the formation of heteromeric complexes or the exhibition of a novel pharmacology. The activity of particular G protein linked second messenger systems, such as adenylyl cyclase, is consistent with the postulate that M_2 and M_3 muscarinic receptor subtypes interact with multiple G proteins in CHO cells.

Acknowledgments

This work was supported by NIH Grant NS30882.

References

[1] Arunlakshana O, Schild HO. Some quantitative uses of drug antagonists. Br J Pharmacol 1959;14:48–58.
[2] Jordan BA, Devi LA. G-protein-coupled receptor heterodimerization modulates receptor function. Nature 1999;399:697–700.
[3] Eglen RM, Hegde SS, Watson N. Muscarinic receptor subtypes and smooth muscle function. Pharmacol Rev 1996;48:531–65.
[4] Ehlert FJ, Thomas EA, Gerstin EH, Griffin MT. Muscarinic receptors and gastrointestinal smooth muscle. In: Eglen RM, editor. Muscarinic receptor subtypes in smooth muscle. Boca Raton: CRC Press; 1997. p. 92–147.
[5] Ehlert FJ, Griffin MT, Glidden PF. The interaction of the enantiomers of aceclidine with subtypes of the muscarinic receptor. J Pharmacol Exp Ther 1996;279:1335–44.
[6] Thomas EA, Hsu HH, Griffin MT, Hunter AL, Luong T, Ehlert FJ. Conversion of *N*-(2-chloroethyl)-4-piperidinyl diphenylacetate (4-DAMP mustard) to an aziridinium ion and its interaction with muscarinic receptors in various tissues. Mol Pharmacol 1992;41: 718–26.
[7] Candell LM, Yun SH, Tran LL, Ehlert FJ. Differential coupling of subtypes of the muscarinic receptor to adenylate cyclase and phosphoinositide hydrolysis in the longitudinal muscle of the rat ileum. Mol Pharmacol 1990;38:689–97.
[8] Berridge MJ, Downes CP, Hanley MR. Lithium amplifies agonist-dependent phosphatidylinositol responses in brain and salivary glands. Biochem J 1982;206:587–95.
[9] Kendall DA, Hill SJ. Measurement of [^{3}H]inositol phospholipid turnover. In: Yamamura HI, editor. Methods in neurotransmitter receptor analysis. New York: Raven Press; 1990. p. 68–87.
[10] Schultz J, Hamprecht B, Daly JW. Accumulation of adenosine 3′:5′-cyclic monophosphate in clonal glial cells: labeling of intracellular adenine nucleotides with radioactive adenine. Proc Natl Acad Sci USA 1972;69:1266–70.
[11] Gharagozloo P, Lazareno S, Popham A, Birdsall NJ. Allosteric interactions of quaternary strychnine and brucine derivatives with muscarinic acetylcholine receptors. J Med Chem 1999;42:438–45.
[12] Ehlert FJ, Oliff HS, Griffin MT. The quaternary transformation products of *N*-(3-chloropropyl)-4-piperidinyl diphenylacetate and *N*-(2-chloroethyl)-4-piperidinyl diphenylacetate (4-DAMP mustard) have differential affinity for subtypes of the muscarinic receptor. J Pharmacol Exp Ther 1996;276:405–10.
[13] Esqueda EE, Gerstin Jr EH, Griffin MT, Ehlert FJ. Stimulation of cyclic AMP accumulation and phosphoinositide hydrolysis by M_3 muscarinic receptors in the rat peripheral lung. Biochem Pharmacol 1996;52:643–58.
[14] Peralta EG, Ashkenazi A, Winslow JW, Ramachandran J, Capon DJ. Differential regulation of PI hydrolysis and adenylyl cyclase by muscarinic receptor subtypes. Nature 1988;334:434–7.
[15] Michell RH. Inositol phospholipids and cell surface receptor function. Biochim Biophys Acta 1975;415:81–147.
[16] Birdsall NJ, Hulme EC, Keen M. The binding of pirenzepine to digitonin-solubilized muscarinic acetylcholine receptors from the rat myocardium. Br J Pharmacol 1986;87:307–16.
[17] Birdsall NJ, Farries T, Gharagozloo P, Kobayashi S, Lazareno S, Sugimoto M. Subtype-selective positive cooperative interactions between brucine analogs and acetylcholine at muscarinic receptors: functional studies. Mol Pharmacol 1999;55:778–86.
[18] Michal P, Lysíková M, Tucek S. Dual effects of muscarinic M_2 acetylcholine receptors on the synthesis of cyclic AMP in CHO cells: dependence on time. Br J Pharmacol 2001;132:1217–28.
[19] Gao BN, Gilman AG. Cloning and expression of a widely distributed (type IV) adenylyl cyclase. Proc Natl Acad Sci USA 1991;88:10178–82.
[20] Feinstein PG, Schrader KA, Bakalyar HA, Tang W-J, Krupinski J, Gilman AG, Reed RR. Molecular cloning and characterization of a Ca^{2+}/calmodulin-insensitive adenylyl cyclase from rat brain. Proc Natl Acad Sci USA 1991;88:10173–7.
[21] Sutkowski EM, Tang W-J, Broome CW, Robbins JD, Seamon KB. Regulation of forskolin interactions with type I, II, V, and VI adenylyl cyclases by $G_{s\alpha}$. Biochemistry 1994;33:12852–959.
[22] Tang WJ, Gilman AG. Type-specific regulation of adenylyl cyclase by G protein $\beta\gamma$ subunits. Science 1991;254:1500–3.
[23] Ashkenazi A, Winslow JW, Peralta EG, Peterson GL, Schimerlik MI, Capon DJ, Ramachandran J. An M_2 muscarinic receptor subtype coupled to both adenylyl cyclase and phosphoinositide turnover. Science 1987;238:672–5.
[24] Lazareno S, Gharagozloo P, Kuonen D, Popham A, Birdsall NJ. Subtype-selective positive cooperative interactions between brucine analogues and acetylcholine at muscarinic receptors: radioligand binding studies. Mol Pharmacol 1998;53:573–89.
[25] Maggio R, Barbier P, Colelli A, Salvadori F, Demontis G, Corsini GU. G protein-linked receptors: pharmacological evidence for the formation of heterodimers. J Pharmacol Exp Ther 1999;291:251–7.
[26] Barbier P, Colelli A, Bolognesi ML, Minarini A, Tumiatti V, Corsini GU, Melchiorre C, Maggio R. Antagonist binding profile of the split chimeric muscarinic M_2-trunc/M_3-tail receptor. Eur J Pharmacol 1998;355:267–74.